POSTER REFERENCE: ICF100507PR

FRACTURE PREDICTIONS FOR DUCTILE STEEL

G. Pape*, A. Bakker* and M. Janssen*

* Delft University of Technology, Laboratory of Materials Science,
Rotterdamseweg 137, 2628 AL, Delft, The Netherlands

ABSTRACT

Ductile failure predictions have been made for several geometries of notched and smooth tensile specimen. Ductile damage has been accounted for in these predictions using a local failure criterion. This criterion, a Rice & Tracey [1] model for the growth of voids in a triaxial stress field gives a prediction of the relative enlargement of an imperfection with initial radius R_0. Experimental results have been used to compare with numerical predictions of fracture initiation. Damage has been evaluated in every material location as a continuous distribution of a scalar variable. The model has underestimated local damage in the notched tensile specimen. Introduction of a length parameter in the damage calculation accounts for microstructural effects and an appropriate length scale can be related to inclusion distances in the material. Analysing the physical damage in a smooth tensile specimen prior to failure will reveal early stages of fracture initiation. If failure initiates at macroscopic level (small crack) prior to specimen failure, this would result in a better agreement between numerical predictions of ductile damage and results from experiments. A more critical approach was used using the Rice and Tracey damage model. A comparison have been made for smooth round, smooth square and flat notched specimen. The area reduction at fracture has been compared with numerical predictions. These geometries show unexplained discrepancy between numerical predictions and experimental results.
The influence of the strain rate has been taken into account in the numerical simulations by incorporating a strain rate dependent material behaviour derived from experimental data. Only small reductions of the failure strain were calculated using this approach and this compares rather well to experimental results.

KEY WORDS

Ductile Damage, Local Fracture Criterion, Experiments, Numerical Prediction

INTRODUCTION

Research for the Royal Netherlands Navy on the vulnerability of warships has resulted in a detailed study on the failure behaviour of explosively loaded panels inside ship structures. This study contains on the one hand a determination of the material response to high strain rate deformation, and on the other hand an investigation of the failure behaviour of the material. This paper is concerned with experimental and numerical failure investigations of the material; also the influence of the strain rate has been taken into

account. The experimental determination of the flow stress has been presented in an additional paper [2]. First some experiments will be described and results will be presented. Numerical simulations of the experiments including ductile damage have been presented in the next section. Two approaches for failure predictions will be discussed and attention will be paid to the influence of the strain rate on the failure behaviour. Finally, conclusions have been drawn and recommendations for further research have been made.

FRACTURE EXPERIMENTS ON NOTCHED SPECIMEN

The influence of hydrostatic stresses on the failure behaviour of steel has been investigated experimentally. For several geometries of tensile specimen the load-displacement curves have been recorded and the area reduction at failure has been measured. Flat tensile specimen witch notches on both sides have been applied for this research. To vary the level of hydrostatic stress in the specimen, several notch radii have been applied. The influence of the rolling direction of the plate material has been investigated as well as the influence of the strain rate on the failure strain. Figure 1 shows the dimensions of the notched tensile specimen, for high strain rates the specimen width was increased to 15 mm and the gauge length L to 90 mm, also the clamping parts have been modified. This change was made in order to maintain pure elastic deformation outside the notch region.

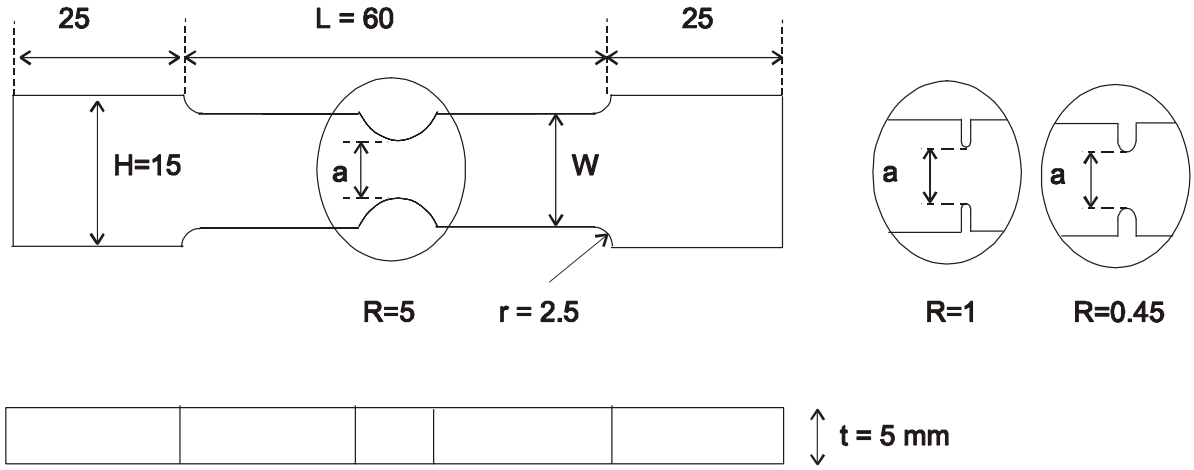

Figure 1: Dimensions of notched specimen [mm]. Notches with radii R=5 mm, 1 mm, and 0.45 mm have been used, a = 5 mm, W = 10 mm.

For low strain rates the experimental curves of load versus displacement have been shown in Figure 2 for three different notch radii. The local strain rate at the notch tip has been calculated using the finite element method and varied from 6.10^{-4} s^{-1} to 1.10^{-3} s^{-1} for these experiments. Displacements have been measured using a strain gauge extensometer with a gauge length of 37.5 mm. As the region outside the notch deforms only elastically, the elongation mainly arises from plastic deformation at the notch. In the figure also arrows have indicated the points of initiation of fracture. A specimen with a notch radius of 0.45 mm was broken in a brittle way just after this initiation point and showed small ductile initiation of fracture at the notch tip. The increase of the maximum load is thought to be caused by increasing hydrostatic stress level at the notch. The area reduction at failure strongly decreases with increasing load level, and this confirms the assumption that hydrostatic stress enhances ductile failure. Figure 3 shows the average values of the failure strain from area reduction at fracture measured from several experiments, and have been computed from:

$$\varepsilon_f = \ln\left(\frac{A_0}{A_f}\right) \tag{1}$$

in which ε_f is the true fracture strain and A_0 and A_f the initial and fracture cross sectional area at the notch, respectively. Several strain rates have been applied in the rolling direction of the material (indicated by curves) and the strain rates in the graph were derived using the finite element method. The influence of the rolling direction is remarkably high compared to the strain rate influence and has been tested only at low strain rates for specimen perpendicular to the rolling direction of the plate material (single points).

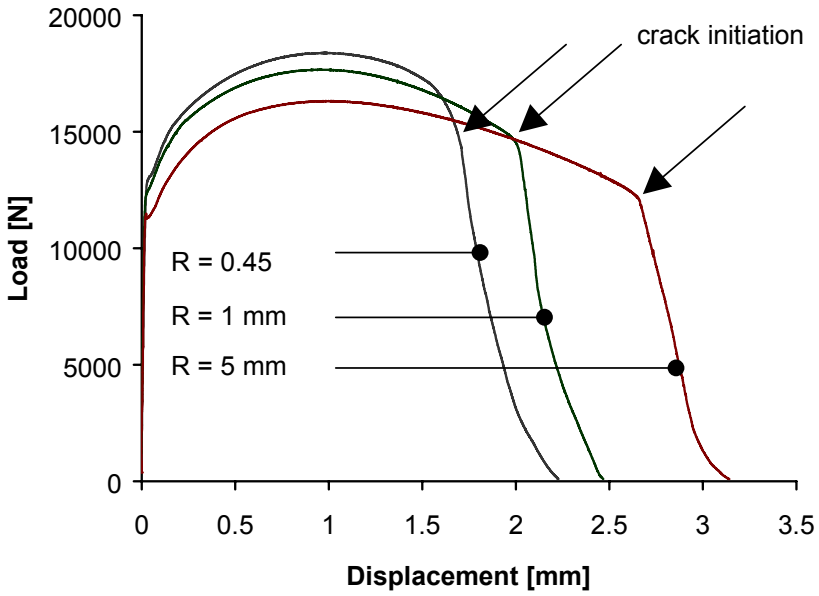

Figure 2: Load – displacement curves for notched specimen in the rolling direction of the plate material at low tensile velocity. Notch radii have been indicated by R.

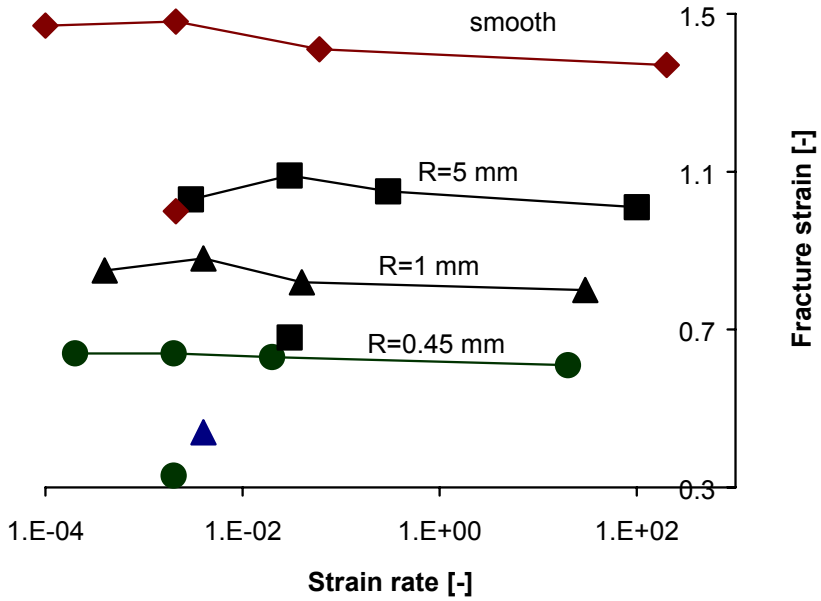

Figure 3: Fracture strains from area reduction for smooth and notched specimen at several strain rates. Strain rates are average values related to area reductions. Standard deviations vary from 0.02 to 0.05.

NUMERICAL PREDICTIONS OF DUCTILE FAILURE

Damage Predictions According to Rice and Tracey

Numerical simulations have been performed using the flow stress of the material, which has been determined experimentally, [2]. The flow stress has been defined as a function of the plastic strain and strain rate. Three-dimensional models have been used to model 1/8 part of each notched specimen, taking into account symmetry conditions. Also a smooth round tensile specimen of 5 mm diameter has been simulated. A preliminary analysis showed that the influence of mass inertia effects is negligible and therefore no dynamic effects have been incorporated into the analysis. A standard plasticity algorithm has been used in the finite element calculations, together with a von Mises yield criterion and isotropic strain hardening. The Rice and Tracey model for ductile damage evolution has been incorporated. The model describes the growth of a void in a plastically deforming material. Assuming an initial void radius R_0 the growth has been given by:

$$\ln\left(\frac{R}{R_0}\right) = 0.283 \cdot \int_{\varepsilon_p} \exp(A_{RT} \cdot \sigma_h / \sigma_e) \quad d\varepsilon_p \tag{2}$$

in which A_{RT} is a constant equal to 3/2, σ_h the hydrostatic stress and σ_e the equivalent von Mises stress. Some results of finite element calculations at low strain rates will be discussed first.

Figure 4 shows local values of the relative hydrostatic stress (triaxiality) σ_h / σ_e . These values have been evaluated at the position of maximum damage, for the R = 1 mm and R = 0.45 mm radius specimen this is at the centre of the notch tip and for the R = 5 mm and smooth specimen at the centre of the minimum cross section. For the specimen with radius R = 1 mm is not quite clear if the initiation position is at the centre of the specimen or at the notch tip. This will be investigated experimentally in the future. As a criterion to stop the numerical simulations the failure strain according to Eqn. 1 has been used. Numerically, the strain from area reduction at the notch equals the experimental fracture strain when the calculation stops.

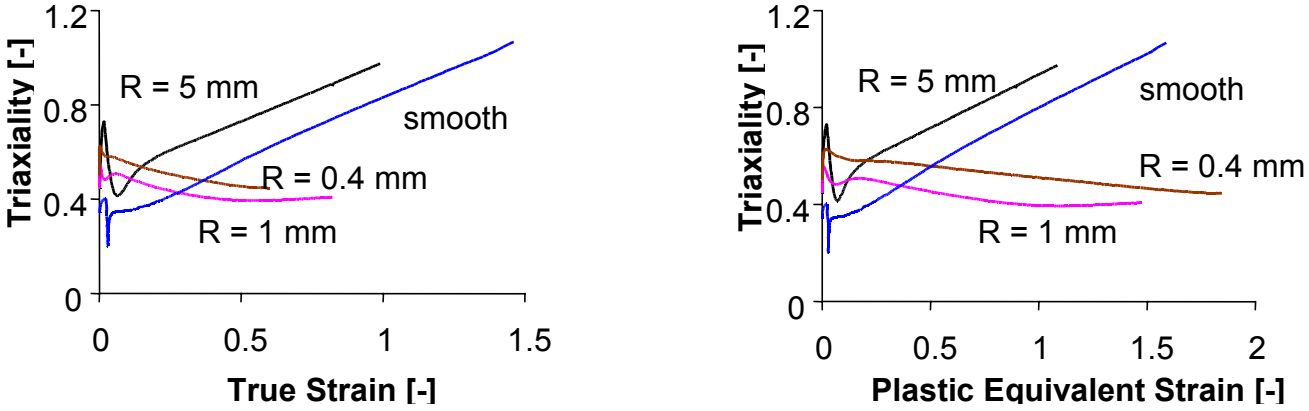

Figure 4: Triaxialities for several geometries at low strain rates. Notched geometries have been indicated by specifying the notch radius R, round tensile specimen is indicated by "smooth". Left figure (a) uses strain from area reduction, right figure (b) uses local plastic strain.

The calculated damage evolution according to Eqn. 2 has been shown in Figure 5 at identical positions in the specimen compared to the results shown in Figure 4. Taking into account the relation for ductile damage, Eqn. 2, together with the calculated hydrostatic stress - plastic strain history, Figure 4, one can conclude that no accordance can be achieved for the smooth and notched R = 5 mm specimen. This applies also for the R = 1 mm and R = 0.45 mm notched specimen. This conclusion becomes clear from Figure 5.

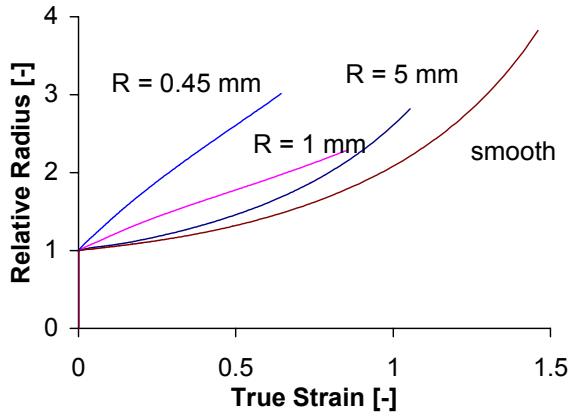

Figure 5. Relative radius predictions according to Rice and Tracey, $A_{RT} = 3/2$.

Influence of the Strain Rate

The damage predictions presented in this work do not include a dependence of the strain rate directly. This can be seen from the formulation used for local failure prediction, Eqn. 2. Implicitly this mechanism is accounted for by strain rate dependence of the flow stress. Experimental results confirmed the choice of this relatively simple approach. No significant dependence of the fracture characteristics has been observed from the tensile tests at different rates of strain. Elongation, reduction of area at fracture, and fracture surface showed no remarkable changes at elevated strain rates. A minor reduction of strain from area reduction might be concluded.

The influence of the strain rate on the local damage prediction in quasi-static analyses has been investigated as well. In these analyses the mass inertia influence has been neglected. In these analyses the strain rate influences the flow stress and will result in strain rate dependent damage evolution. However, physical processes that might influence the void growth on a different basis than the influence of the strain rate on the flow stress have not been taken into account. Reduction of strain at failure has been predicted from the numerical results, applying the same critical damage value for all strain rates. For an increase of the strain rate of 1.10^5 s^{-1} the failure strain reduces about 0.1 for the smooth specimen and about 0.06 for all notched geometries. These values agree with the experimental observations.

Introduction of a Length Parameter

Failure predictions using a characteristic volume might improve the analogy between experimental results and numerical computations. This volume represents a certain process zone in which failure takes place. The characteristic length of the zone can be related to microstructural characteristics, such as the average inclusion size or grain size. The finite element model has been chosen is such a way that the element length in front of the notch tip is equal for all notched specimens. Damage has been evaluated as the average value of each element. As the formulation for strain calculation uses an updating of the incremental displacements (Updated Lagrange), the elements deform in a similar way as the material structure. This can be interpreted as to account for the changing inter-inclusion spacing at proceeding deformation. The element length has been chosen in such a way that the model size would not be excessively large. This element length is approximately 210 µm and might be related to the average inclusion distance of the manganese sulphides, which has been estimated to be 310 µm.

The critical damage value from a smooth tensile specimen changes not significantly using the constant element size approach, as the gradient in damage is small in the specimen centre. A calculation has been performed applying constant element size with similar dimensions as has been used for the notched specimen. From this calculation a damage value of 3.7 has been found. From the finite element results can be concluded that fracture initiation in the notched specimens takes place at lower damage values compared with the smooth tensile specimen. Taking a closer look to the damage curves, the critical value of the relative radius at failure initiation is approximately 2.5 ± 0.35 for all notched geometries. For the smooth specimen this relative void radius corresponds to a strain of 1.2 ± 0.1. Interrupted tests have been

analysed to gain more insight in the process of ductile fracture initiation in the smooth specimen. Table 1 shows the predicted area strains together with experimental results at low strain rates for a critical R/R_0 value of 2.5.

TABLE 1
COMPARISON OF NUMERICAL PREDICTIONS WITH EXPERIMENTAL VALUES
FOR STRAIN FROM AREA REDUCTION AT FAILURE INITIATION.

	smooth	R = 5 mm	R = 1 mm	R = 0.45 mm
experiment	1.47	0.9 – 1.03	0.75 – 0.85	0.55 – 0.64
prediction	1.2	0.97	0.87	0.44

For the notched geometries a more consistent prediction of failure has been obtained. For all notch geometries a damage value of 2.5 has been obtained at fracture initiation. Smooth specimen modelling still results in a larger damage value at failure compared with notched specimen. An approximate failure criterion has been found however, underestimating the failure strain for a smooth specimen with a relative error of 20%. Considering energy absorption in the last stage of deformation prior to fracture of the specimen, this inaccuracy is acceptable.

CONCLUSIONS & RECOMMENDATIONS

From the experimental results has been observed that the failure strain from area reduction at fracture does not change significantly with the strain rate. In a first approximation this effect might be neglected. A decreasing notch radius also decreases the failure strain and increases the hydrostatic stress at the notch. A large influence has been found of the rolling direction of the plate material. The failure strain decreases strongly in the direction perpendicular to the rolling direction.
Application of a ductile damage model according to Rice and Tracey results in inconsistent damage predictions at the experimentally determined fracture strain from area reduction. This is inherent to the applied formulation taking into account the triaxiality – plastic strain path for the points where fracture initiates. Another approach where a certain element volume has been taken into account results in consistent failure predictions for the notched specimen. Comparing this damage prediction at failure with a smooth specimen, an overestimation of damage has been found from the numerical results. However, this approach can be used for a first approximation of the failure behaviour of blast loaded panels in ship structures.

A comparison of void sizes for a notched specimen with notch radius R = 5 mm and a smooth specimen before the onset of failure would be interesting, relating these values to finite element predictions.

ACKNOWLEDGEMENTS

This research was funded by the Technology Foundation STW, the TNO Prins Maurits Laboratory and the Delft University of Technology.

REFERENCES

1. Rice, J.R., Tracey, D.M., (1969) *On the Ductile Enlargement of Voids in Triaxial Stress Fields*, Journal of the Mechanics and Physics of Solids, vol. 17, 201
2. Pape, G., Bakker, A., Janssen, M., (2001) *Flow Stress of Steel at Large Strains and High Strain Rates*, International Conference on Fracture, ICF 10, Conference Proceedings, Honolulu